



# The Synthesis of Lead-Free Ferroelectric $\text{Bi}_{1/2}\text{Na}_{1/2}\text{TiO}_3$ Thin Film by Solution-Sol-Gel Method

CHANG-YEOUL KIM\*

*Korea Institute of Ceramic Engineering and Technology, 233-5, Kasan-dong Keum Cheon-ku, 153-801, Seoul, Korea*  
cykim15@kicet.re.kr

TOHRU SEKINO, YO YAMAMOTO AND KOICHI NIIHARA

*The Institute of Scientific and Industrial Research, Osaka University, 8-1 Mihogaoka Ibaraki, 567-0047, Osaka, Japan*

*Received January 20, 2004; Accepted August 18, 2004*

**Abstract.**  $\text{Bi}_{1/2}\text{Na}_{1/2}\text{TiO}_3$  (described as BNT) is considered as a promising lead-free ferroelectric material. In this study, BNT sol was synthesized by mixing bismuth oxide and sodium carbonate dissolved in nitric acid and titanium tetraisopropoxide in ethylene glycol, which was called a solution-sol-gel method and very cost-effective synthesis method, while very high-cost metal alkoxides are used as precursors in conventional sol-gel method. FT-IR and Raman analyses indicated that the chemical modification of titanium tetraisopropoxide by glycolic acid or oxalic acid occurred and the synthesis of stable BNT sol was possible. In the results of high temperature X-ray analysis and DTA/TG analyses, the crystallization of BNT was thought to occur at between 500 and 700°C following the evaporation of solvent and organics and poly-condensation processes. The main crystal phase of the film was identified as rhombohedral crystal phase of  $\text{Bi}_{1/2}\text{Na}_{1/2}\text{TiO}_3$  by XRD and Raman spectroscopy analyses, although a small amount of  $\text{Bi}_4\text{Ti}_3\text{O}_{12}$  existed as a second phase.

**Keywords:** lead-free, ferroelectric, solution-sol-gel, chemical modification, crystallization

## 1. Introduction

Since  $\text{Bi}_{1/2}\text{Na}_{1/2}\text{TiO}_3$  (described as BNT) was first synthesized by Smolensky et al. [1], it has attracted attention as a promising lead-free ferroelectric material. The pyroelectric and piezoelectric properties of  $\text{Bi}_{1/2}\text{Na}_{1/2}\text{TiO}_3$  single crystals and sintered ceramics were widely studied. Takenaka et al. [2] reported that BNT-BaTiO<sub>3</sub> has piezoelectric constant  $d_{33} = 125$  ( $10^{-12}$  C/N). There are reports about the superstructure of BNT [3, 4], phase relations of  $(\text{Bi}_{1/2}\text{K}_{1/2})\text{TiO}_3$ - $(\text{Bi}_{1/2}\text{Na}_{1/2})\text{TiO}_3$  system [5],  $(\text{Bi}_{1/2}\text{Na}_{1/2})\text{TiO}_3$ -PbTiO<sub>3</sub> system [6], BNT single crys-

tal and  $(\text{Bi}_{1/2}\text{Na}_{1/2})_{(1-1.5x)}\text{La}_x\text{TiO}_3$  [7, 8]. However, there has been no report of the synthesis of the BNT thin film by sol-gel method.

The solution-sol-gel method applied in this study is a little different from traditional sol-gel processing. In traditional sol-gel processing, metal alkoxides are used as precursors for synthesis of oxide powder or thin film. In this research, however, bismuth oxide and sodium carbonate was dissolved in nitric acid and their solution was used as a precursor along with titanium isopropoxide. In our previous study, it was reported that nano-sized BNT powders could be synthesized by dissolving  $\text{Bi}_2\text{O}_3$  and  $\text{Na}_2\text{CO}_3$  in nitric acid and adding titanium tetraisopropoxide and heat-treating the precursor. When hydrochloric acid was used

\*To whom all correspondence should be addressed.

for the dissolution of  $\text{Bi}_2\text{O}_3$  and  $\text{Na}_2\text{CO}_3$  [9], BNT could not be synthesized because of the formation of second phase of  $\text{BiOCl}$ . In this study, we focused on the investigation of BNT precursor chemistry and the crystallization behavior and microstructural observations of BNT thin films prepared by solution-sol-gel method. It is very important to investigate the chemical modification in the solution-sol-gel processing as a fundamental knowledge for synthesis of BNT thin film. BNT transparent sol was synthesized and its chemical modification was analyzed by FT-IR and Raman spectroscopy. BNT thin film was prepared by spin-coating the transparent sol. The evaporation and polycondensation processes of BNT transparent sol were analyzed by TG-DTA. The crystallization of BNT was also studied by high-temperature X-ray diffraction analysis and Raman spectroscopy. The microstructures of BNT thin film were investigated by using FE-SEM and TEM.

## 2. Experimental Procedure

### 2.1. Synthesis of Transparent Sol by Solution-Sol-Gel Method

Bismuth oxide,  $\text{Bi}_2\text{O}_3$  (Kojundo Chemical Laboratory Co., Ltd., Saitama, Japan, 99.9%, 1–2  $\mu\text{m}$ ) and sodium carbonate,  $\text{Na}_2\text{CO}_3$  (Kojundo Chemical Laboratory Co., Ltd., Saitama, Japan, 99%, anhydrous) were dissolved in nitric acid ( $\text{HNO}_3$ , Wako Pure Chemical Industries Ltd., Osaka, Japan, 69–70%), and this solution was put into ethylene glycol,  $\text{OHCH}_2\text{CH}_2\text{OH}$  (Wako Pure Chemical Industries Ltd., Osaka, Japan, 99.5%). The solution was transparent and precipitation did not occur. Then, a stoichiometric amount of titanium tetraisopropoxide,  $\text{Ti}(\text{OCH}(\text{CH}_3)_2)_4$  (Wako Pure Chemical Industries Ltd., Osaka, Japan, min. 95%) was added to the solution, and the mixture was stirred at 60°C for 1 hr. The concentration ratio of metal ions to ethylene glycol was 1 to 10. After this process, the color turned to transparent yellow. To investigate the sol-gel chemistry of BNT, we analyzed ethylene glycol (EG),  $\text{Bi}_2\text{O}_3$  and  $\text{Na}_2\text{CO}_3$  solution in ethylene glycol, titanium tetraisopropoxide (TTIP) in ethylene glycol, and BNT sol by FT-IR (WINSPEC 100 JEOL, Tokyo, Japan) and Raman spectroscopy (SPEX 1482D, SPEX INDUSTRIES, INC., NJ, USA).

High temperature X-ray diffraction analysis (XRD, Scintag, CA, USA) was carried out to know the crystallization process of BNT from the sol. The BNT sol was first dried at 170°C, and then was put on the plat-

inum plate and analyzed at room temperature, 300, 500, 700, and 900°C after holding at each temperature for 30 min in air by the high temperature X-ray diffraction equipment.

### 2.2. Thin-Film Fabrication by Spin-Coating Method

As a drying control chemical additive (DCCA), a small amount of formamide was added to the stock solution synthesized by solution-sol-gel method [10]. As a result, a yellowish transparent sol was obtained. The sol was spin-coated on Si (100, P-type, about 2–3  $\Omega$ ), at 3000 rpm for 20 s. It was dried on a hot plate at 250°C for 10 min. The process of spin-coating/drying was repeated to get the necessary film thickness. After that, the dried film on silicon wafer was heat-treated at 700°C for 30 min in air in electrical furnace, of which heating rate was 50°C/min.

### 2.3. Characterization of the BNT Thin Film

The crystal phase of the heat-treated film was identified by powder X-ray diffraction method (Model RU-200B, Rigaku Co., Ltd., Tokyo, Japan) and Raman scattering spectroscopy (SPEX1482D, SPEX INDUSTRIES, INC., NJ, USA). For Raman spectroscopy, an Ar laser of 514.5 nm was used. BNT powders sintered at 1150°C for 4 h were used as a reference material for crystal phase identification by XRD analysis and Raman spectroscopy.

The microstructure of the film was observed by scanning electron microscopy (SEM, Model S-5000, Hitachi Co., Ltd., Tokyo, Japan). Cross-sectional microstructure of the thin film and its diffraction pattern were observed by transmission electron microscopy (TEM, Hitachi 8100T, Hitachi Co., Ltd., Tokyo, Japan, 200 kV).

## 3. Results and Discussion

### 3.1. Sol Chemistry

FT-IR spectra of precursors are shown in Fig. 1. When titanium tetraisopropoxide was added to ethylene glycol, the bands at 1130 and 915  $\text{cm}^{-1}$  (solid squares) were observed. These bands were attributed to  $\nu$  (Ti—O—C), and the band of 640  $\text{cm}^{-1}$  (open squares) was attributed to  $\nu$  (Ti—O—C). The bands at 2396, 1762, 1399, and 826  $\text{cm}^{-1}$  (solid triangles) appeared in

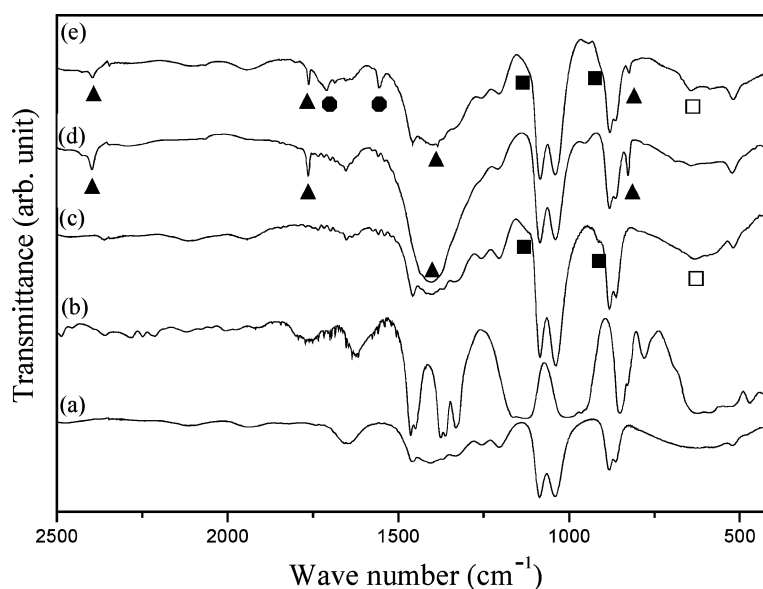


Figure 1. FT-IR spectra of the precursors, ethylene glycol (EG) (a), titanium tetraisopropoxide (TTIP) (b), TTIP in EG (c),  $\text{Bi}_2\text{O}_3$  and  $\text{Na}_2\text{CO}_3$  solution in EG (d), BNT precursor (e).

$\text{Bi}_2\text{O}_3$  and  $\text{Na}_2\text{CO}_3$  solution in ethylene glycol. These bands were attributed to  $\text{Bi}(\text{NO}_3)_3$  and  $\text{NaNO}_3$  vibration mode. It indicates that  $\text{Bi}_2\text{O}_3$  and  $\text{Na}_2\text{CO}_3$  solution in nitric acid existed in the form of  $\text{Bi}(\text{NO}_3)_3$  and  $\text{NaNO}_3$  in precursor solution. In the BNT sol, two new bands appeared at  $1709$  and  $1554 \text{ cm}^{-1}$  (solid circles) which were attributed to  $\nu(\text{COO})$  vibration modes. The appearance of (COO) vibration modes indicates that titanium tetraisopropoxide was modified by oxidation products of ethylene glycol.

The sol-gel processing of  $\text{TiO}_2$  is usually performed via the hydrolysis and polycondensation of titanium

alkoxides in the presence of an acid catalyst. Acids are supposed to increase the lability of protonated OR groups and favor electrophilic substitutions. According to literature [11, 12], three coordination modes of carboxylic acids to a metal atom are known, i.e., monodentate via one oxygen atom, bidentate chelating via both oxygen atoms, and bidentate bridging between two metal atoms, as is shown in Fig. 2. It is suggested from the above FT-IR results that titanium tetraisopropoxide was modified in the form of monodentate or bidentate chelating in ethylene glycol under nitric acid catalyst as is seen in Fig. 3. Ethylene glycol was

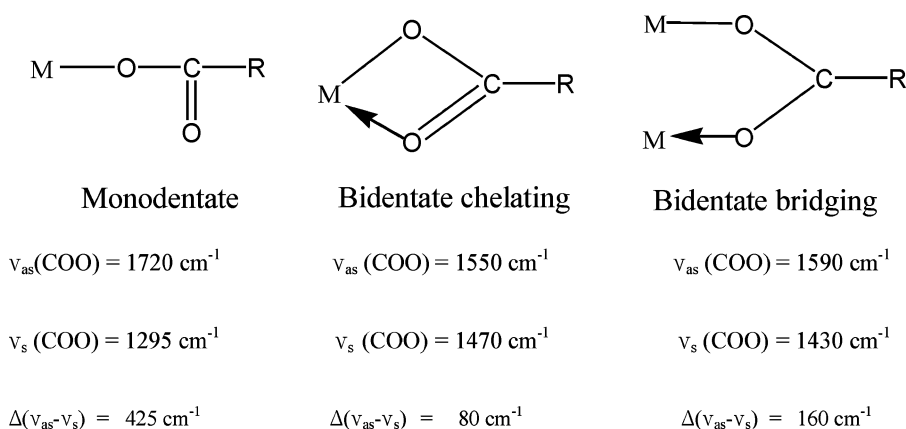


Figure 2. Different coordination modes occurring in metal carboxylates [11].

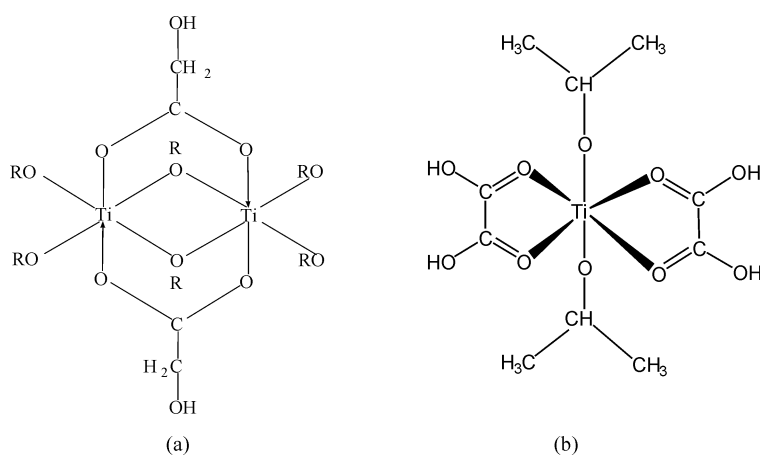


Figure 3. Titanium tetraisopropoxide modified by glycolic acid (a) and oxalic acid (b).

oxidized by nitric acid to glycolic acid and then was converted to oxalic acid upon heating. Figure 3 shows that titanium tetraisopropoxide could be modified by glycolic acid or oxalic acid to have COO vibration mode in BNT precursor sol.

Figure 4 shows the Raman scattering spectra of precursors, ethylene glycol, bismuth oxide and sodium

carbonate solution in ethylene glycol, titanium tetraisopropoxide in ethylene glycol, BNT sol, and BNT gel. In the Raman spectra of bismuth oxide and sodium carbonate solution in ethylene glycol, the vibration bands marked by black-filled circle appeared, which are due to bismuth nitrate and sodium nitrate. The vibration bands marked by arrow were attributed to the (Ti—O)

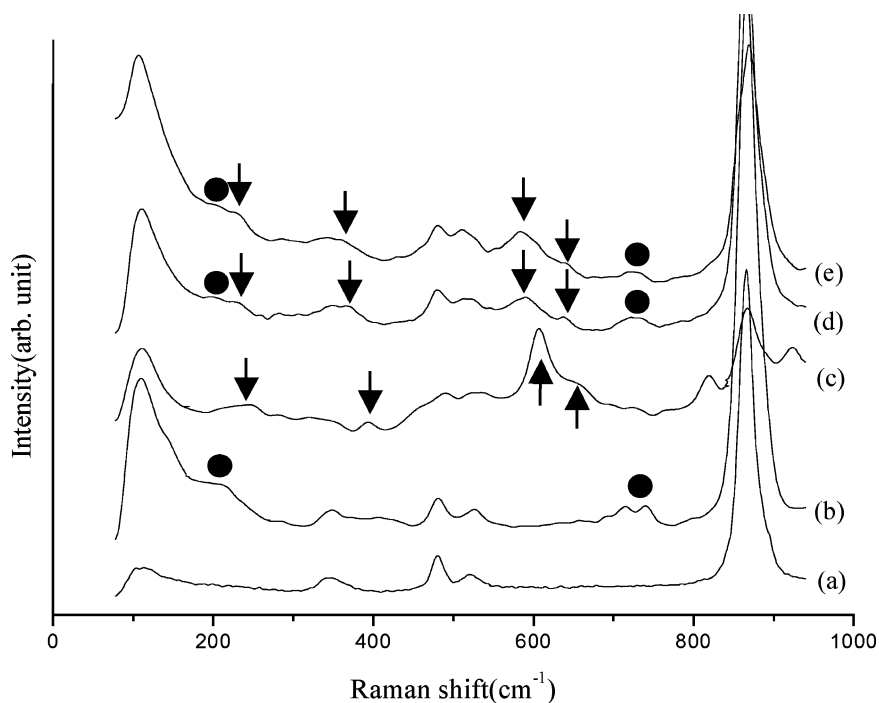


Figure 4. Raman scattering spectra of the precursors. Ethylene glycol (a),  $\text{Bi}_2\text{O}_3$  and  $\text{Na}_2\text{CO}_3$  solution in EG (b), titanium isopropoxide (TIP) in EG (c), BNT sol (d), and BNT gel (e).

vibrations. The vibration bands at  $608$  and  $656\text{ cm}^{-1}$  in titanium tetraisopropoxide were attributed to  $\nu(\text{Ti}-\text{O})$  and were shifted toward  $580$  and  $640\text{ cm}^{-1}$  [13–15]. The peak shift of  $\text{Ti}-\text{O}$  vibration in BNT sol from titanium tetraisopropoxide means that titanium tetraisopropoxide could be modified by ethylene glycol using nitric acid as catalyst. These results are in good agreement with the results of FT-IR analysis of BNT sol.

### 3.2. Thermal Behavior and Crystallization of BNT Precursor

Figure 5 shows the DTA and TG curves for dried BNT sol. Complicated exothermic peaks appeared between  $200$  and  $600^\circ\text{C}$ , and they accompanied weight loss. There was no weight loss above  $600^\circ\text{C}$ . It is thought that the exothermic peaks and weight loss were due to the volatilization of residual solvent and organics and also to the polymerization of BNT precursor. More careful analysis of the TG curves implies that there were four steps of weight decreases. There was about 20% of weight loss to  $230^\circ\text{C}$ , about 64.8% weight loss to  $338^\circ\text{C}$ , 80.8% weight loss to  $484^\circ\text{C}$ , and 94% weight loss to  $600^\circ\text{C}$ . It indicates that BNT crystallization was generated via multiple steps of evaporation of water and solvent, and decomposition and polycondensations of organics [16].

High temperature XRD profiles of dried BNT gel, which was prepared by using nitric acid for dissolving  $\text{Bi}_2\text{O}_3$  and  $\text{Na}_2\text{CO}_3$ , are shown in Fig. 6. It did not show any crystalline peaks at  $500^\circ\text{C}$ , and the BNT crystalline peaks first appeared at  $700^\circ\text{C}$ . The intensity of the peaks increased with increasing temperature up to  $900^\circ\text{C}$ . At  $700^\circ\text{C}$ , there is a broad peak around  $30^\circ$ , showing remaining amorphous phase. However, the crystallization of BNT was found to be finished at  $900^\circ\text{C}$  as seen in Fig. 6.

### 3.3. Crystalline Phase Development of BNT Thin Film

BNT thin film heat-treated at  $700^\circ\text{C}$  for 30 min had the rhombohedral perovskite crystal structure of sodium bismuth titanium oxide (JCPDS 36-0340, peaks marked by filled circle) as shown in Fig. 7. Compared with that of the BNT bulk specimen sintered at  $1150^\circ\text{C}$  for 4 h in air, the BNT thin film was mainly comprised of rhombohedral perovskite crystal phase which we purposed to synthesize, although it contained second phase a little (Fig. 7). The reason of the second phase of pyrochlore crystal formation was not clear at this stage, but it is assumed that it resulted from the reaction of BNT thin film and perhaps because BNT nucleation and crystal growth occurred from the

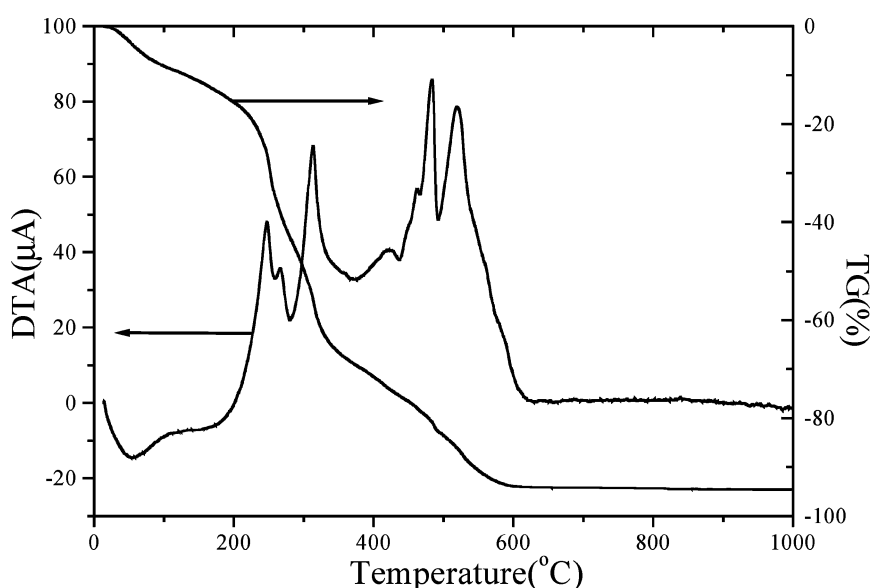


Figure 5. DTA (Differential thermal analysis) and TG (Thermogravimetric analysis) curves of BNT, dried at  $170^\circ\text{C}$ . The heating rate was  $10^\circ\text{C}/\text{min}$  in air.

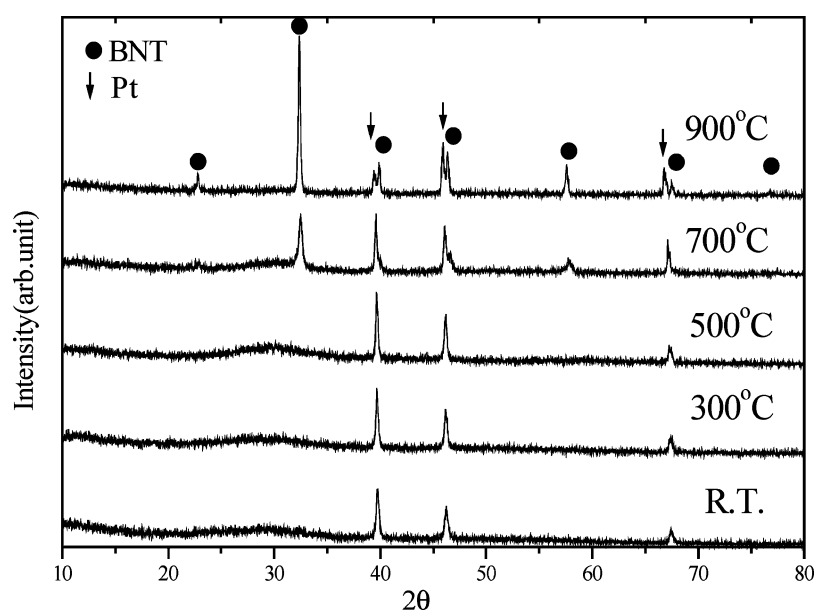


Figure 6. High Temperature X-ray diffraction patterns of BNT powders after drying at 170°C. Pt peaks marked by arrows correspond to the sample holder and heating stage of platinum. Here  $\text{HNO}_3$  was used for dissolving  $\text{Bi}_2\text{O}_3$  and  $\text{Na}_2\text{CO}_3$ .

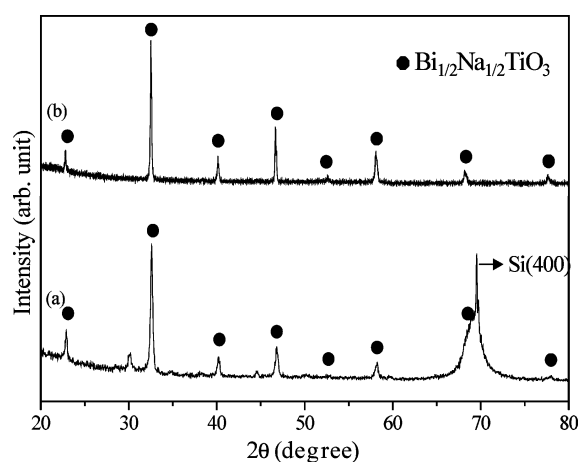


Figure 7. XRD patterns for BNT thin film coated 3 times, dried at 250°C for 10 min., and heat-treated at 700°C for 30 min (a) and BNT body sintered at 1150°C for 4 h using the powder synthesized by solution-sol-gel method (b).

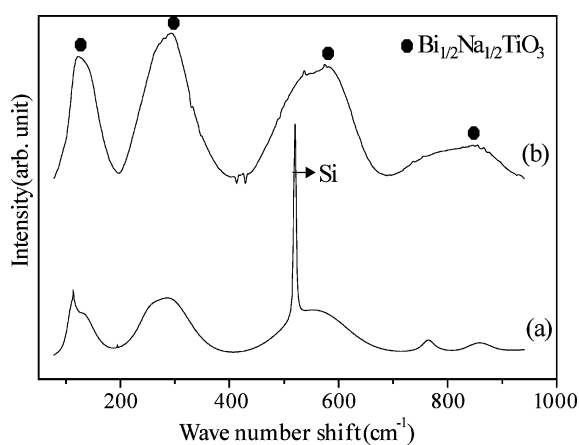


Figure 8. Raman scattering spectra for BNT thin film coated 3 times and heat-treated at 700°C for 30 min (a) and BNT body sintered at 1150°C for 4 h by using the powder synthesized by solution-sol-gel method (b).

amorphous phase, as we will see later at the observation of TEM image.

In the result of Raman spectroscopy in Fig. 8, the BNT thin film heat-treated at 700°C for 30 min showed  $A_1(\text{TO})$  phonon mode of rhombohedral BNT crystal, which is symmetric vibration phonon mode. The Raman bands of the BNT thin film showed almost the

same spectra as those of the sintered body. In Raman spectra of the thin film, Si peak appeared at  $520\text{ cm}^{-1}$  and two unknown peaks also appeared at  $113$  and  $765\text{ cm}^{-1}$ , which are thought to be from second phase of bismuth titanate [17]. The Raman spectra of BNT is related to the crystal structure of  $A_{1/2}^-A_{1/2}^-BO_3$ -type perovskite [18–20]. Considering the paraelectric phase

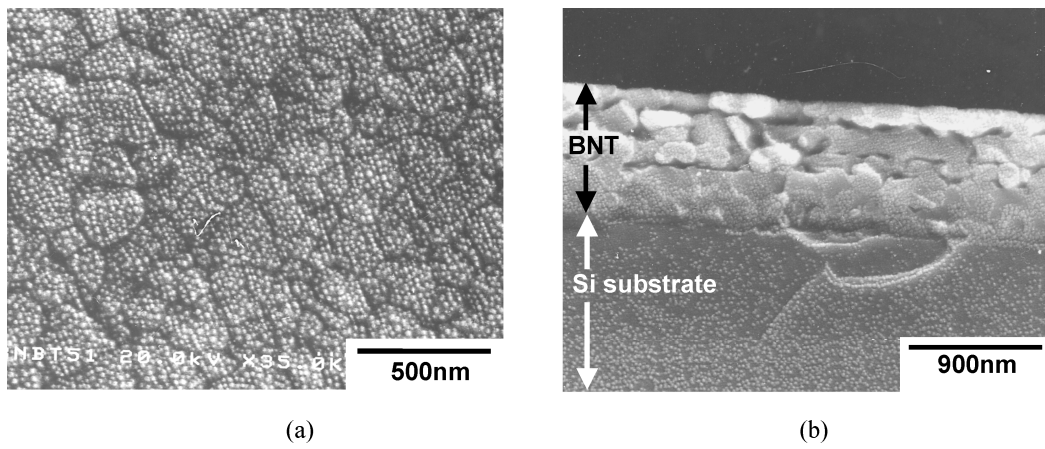


Figure 9. SEM image of BNT thin film which was coated 5 times and heat-treated at 700°C for 30 min. The plane image of BNT thin film (a) and cross section image of the film (b).

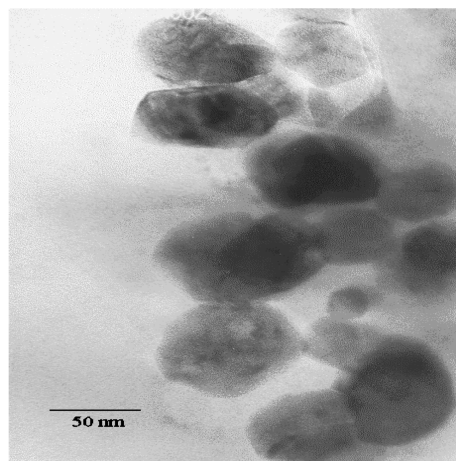
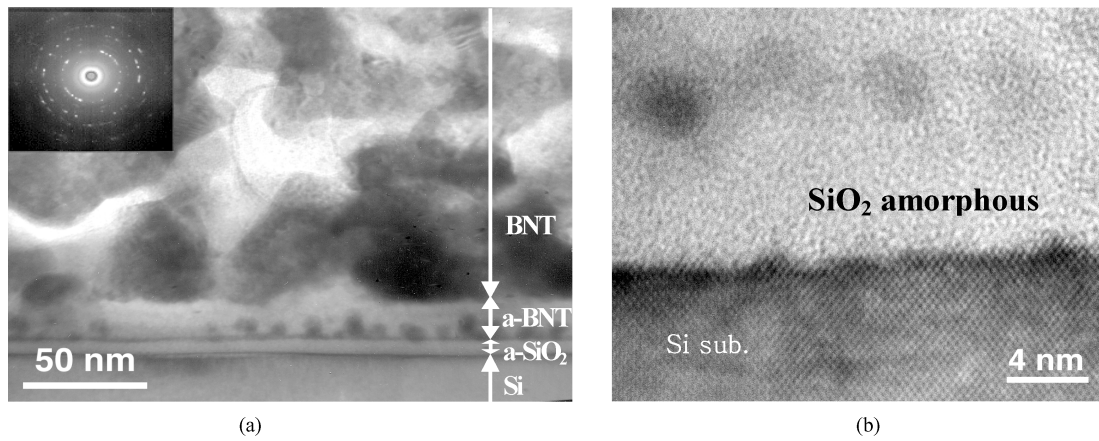


Figure 10. TEM images of BNT thin film which was coated 3 times and heat-treated at 700°C for 30 min. The cross section image of BNT thin film on Si wafer, where a-SiO<sub>2</sub> means amorphous SiO<sub>2</sub> layer and a-BNT is amorphous BNT layer; low magnification (a), high magnification (b), and plane image (c).

of BNT, the structure of BNT has an ordering of alternating Na and Bi ions on the assumption that the space group is  $Fm\bar{3}m$ . Na and Bi ions occupy local positions or sites with an inversion center (a and b positions with the  $m\bar{3}m = O_h$  symmetry); that is also true of the O ions (d positions,  $mmm = D_{2h}$ ), whereas the Ti ions occupy positions without an inversion center (c positions,  $43m = T_d$ ). Siniĭ et al. [19, 20] suggested that the paraelectric phase of BNT consists of microdomains of the ordered  $Fm\bar{3}m$  structure with a minimum size of 10–20 cells at the result of the measurement of half width around  $520\text{ cm}^{-1}$ .

### 3.4. Observations of BNT Thin Film Microstructure

SEM photographs show that the thickness of 2 times coated thin film was 300 nm and that of 5 times coated thin film was 750 nm, from which the thickness of a single coating was estimated as 150 nm (Fig. 9). As is seen in Fig. 9(a), BNT thin film was comprised of about 100 nm-sized homogeneous crystals.

Transmission electron microscopy (TEM) photographs show that the BNT crystal size was about 50–100 nm, and the amorphous phase was found between the BNT film and the silicon wafer (Fig. 10). Two layers of amorphous phase existed; the lower amorphous layer is thought to be amorphous silicon oxide ( $a\text{-SiO}_2$ ) layer due to the thermal oxidation of silicon, and the upper layer is considered to be amorphous BNT ( $a\text{-BNT}$ ) phase that contained nano-sized crystals. The thickness of amorphous silicon oxide layer on silicon wafer is about 7 to 10 nm. We presume that BNT nuclei formed in the amorphous BNT matrix, after which crystal growth occurred. The precise mechanism of BNT crystallization needs further study.

## 4. Conclusions

Lead-free ferroelectric BNT thin films were successfully synthesized by solution-sol-gel method. In this study, stable BNT sol could be synthesized by using inexpensive raw materials of bismuth oxide and sodium carbonate dissolved in nitric acid and titanium tetraisopropoxide. It was found that the chemical modification of titanium tetraisopropoxide by glycolic acid or oxalic acid under nitric acid played very important role in forming a stable sol. DTA/TG analyses and high-temperature XRD results showed that BNT

crystallization started at about  $600^\circ\text{C}$  and was completed at  $900^\circ\text{C}$  through evaporation and condensation processes. The crystal structure of BNT thin film on silicon substrate was identified as rhombohedral  $\text{Bi}_{1/2}\text{Na}_{1/2}\text{TiO}_3$  phase by XRD and Raman spectroscopy. SEM and TEM observations showed that BNT thin films were comprised of 50–100 nm-sized crystals.

## Acknowledgments

The authors are grateful to Japanese Monbusho Ministry for the financial support of this research.

## References

1. G.S. Smolensky, V.A. Isupov, A.I. Agranovskaya, and N.N. Krainik, *Soviet Physics-Solid State* **2**, 2651 (1961).
2. Tadashi Takenaka, Kei-ichi Maruyama, and Koichiro Sakata, *Jpn. J. Appl. Phys.* **30**, 2236 (1991).
3. Seung-Eek Park and Su-Jin Chung, *J. Am. Ceram. Soc.* **77**, 2641 (1994).
4. A.N. Soukhojak, H. Wang, G.W. Farrey, and Y.-M. Chiang, *J. Phys. Chem. Solids* **61**, 301 (2000).
5. Y. Yamada, T. Akutsu, H. Asada, K. Nozawa, S. Hachiga, T. Kurosaki, O. Ikagawa, H. Jujiki, K. Hozumi, T. Kawamura, T. Amakwa, K. Hirota, and T. Ikeda, *Jpn. J. Appl. Phys.* **34**, 5462 (1995).
6. Seung-Eek Park and Kug Sun Hong, *J. Appl. Phys.* **79**, 383 (1996).
7. Y.M. Chiang, G.W. Farrey, and Andrey N. Soukhojak, *Appl. Phys. Lett.* **73**, 3683 (1998).
8. Aree Herabut and A. Safari, *J. Am. Ceram. Soc.* **80**, 2954 (1997).
9. Chang Yeoul Kim, Tooru Sekino, and Koichi Niihara, *J. Am. Ceram. Soc.* **86**, 1464 (2003).
10. L. Hench and G. Orcel, *J. Non-Cryst. Solids* **79**, 177 (1986).
11. S. Doeuff, M. Henry, C. Sanchez, and J. Livage, *J. Non-Cryst. Solids* **89**, 206 (1987).
12. R. Urlaup, U. Posset, and R. Thull, *J. Non-Cryst. Solids* **265**, 276 (2000).
13. M. Arima, M. Kakihana, Y. Nakamura, M. Yahima, and M. Yoshimura, *J. Am. Ceram. Soc.* **79**, 2847 (1996).
14. J. Guilment, O. Poncelet, J. Rigola, and S. Tuchet, *Vibration. Spectr.* **11**, 37 (1996).
15. M. Payne and K. Berglund, *Mat. Res. Soc. Symp. Proc.* **73**, 627 (1986).
16. D. Hennings and W. Mayr, *J. Solid State Chem.* **26**, 329 (1978).
17. A.V. Prasada Rao, A.I. Robin, and S. Komarneni, *Mater. Lett.* **28**, 469 (1996).
18. M.S. Zhang, J.P. Scott, and J.V. Zvirgzde, *Ferroelectr. Lett.* **6**, 147 (1986).
19. I.G. Siniĭ, T.A. Smirnova, and T.V. Kruzina, *Sov. Phys. Solid State* **33**, 61 (1991).
20. I.G. Siny, T.A. Smirnova, and T.V. Kruzina, *Ferroelectrics* **124**, 207 (1991).